Journal Pre-proof


# Class IV lasso peptides synergistically induce proliferation of cancer cells and sensitize them to doxorubicin

Jaime Felipe Guerrero-Garzón, Eva Madland, Martin Zehl, Madhurendra Singh, Shiva Rezaei, Finn L. Aachmann, Gaston Courtade, Ernst Urban, Christian Rückert, Tobias Busche, Jörn Kalinowski, Yan-Ru Cao, Yi Jiang, Cheng-lin Jiang, Galina Selivanova, Sergey B. Zotchev

PII: S2589-0042(20)30982-2

DOI: https://doi.org/10.1016/j.isci.2020.101785

Reference: ISCI 101785

To appear in: *ISCIENCE*

Received Date: 9 July 2020

Revised Date: 16 October 2020

Accepted Date: 5 November 2020

Please cite this article as: Guerrero-Garzón, J.F., Madland, E., Zehl, M., Singh, M., Rezaei, S., Aachmann, F.L., Courtade, G., Urban, E., Rückert, C., Busche, T., Kalinowski, J., Cao, Y.-R., Jiang, Y., Jiang, C.-l., Selivanova, G., Zotchev, S.B., Class IV lasso peptides synergistically induce proliferation of cancer cells and sensitize them to doxorubicin, *ISCIENCE* (2020), doi: https://doi.org/10.1016/j.isci.2020.101785.

# Class IV lasso peptides synergistically induce proliferation of cancer cells and sensitize them to doxorubicin

Jaime Felipe Guerrero-Garzón[1,‡], Eva Madland[2,‡], Martin Zehl[3], Madhurendra Singh[4], Shiva Rezaei[4,5], Finn L. Aachmann[2], Gaston Courtade[2], Ernst Urban[6], Christian Rückert[7], Tobias Busche[7], Jörn Kalinowski[7], Yan-Ru Cao[8], Yi Jiang[8], Cheng-lin Jiang[8], Galina Selivanova[4]*, Sergey B. Zotchev[1]*

[1]Department of Pharmacognosy, University of Vienna, 1090 Vienna, Austria; [2]NOBIPOL, Department of Biotechnology and Food Science, NTNU Norwegian University of Science and Technology, 7034 Trondheim, Norway; [3]Department of Analytical Chemistry, Faculty of Chemistry, University of Vienna, 1090 Vienna, Austria; [4]Department of Microbiology, Tumor and Cell Biology, Karolinska Institutet, 17165 Stockholm, Sweden; [5]Department of Animal Biology, Faculty of Natural Sciences, University of Tabriz, Tabriz, Iran; [6]Department of Pharmaceutical Chemistry, University of Vienna, 1090 Vienna, Austria; [7]Center for Biotechnology, Bielefeld University, Universitätsstraße 27, 33615 Bielefeld, Germany; [8]Yunnan Institute of Microbiology, Yunnan University, 650091 Kunming, P.R.China.

‡ These authors contributed equally to this work.

**Keywords**: Actinomycete bacterium, genome mining, class IV lasso peptides, proliferation of cancer cells, doxorubicin.

*__Corresponding authors__: Sergey B. Zotchev, Email: sergey.zotchev@univie.ac.at; Galina Selivanova, Email: galina.selivanova@mtc.ki.se

**Lead Contact:** Sergey B. Zotchev, Email: sergey.zotchev@univie.ac.at

## SUMMARY

Heterologous expression of a biosynthesis gene cluster from *Amycolatopsis* sp. resulted in the discovery of two unique class IV lasso peptides, felipeptins A1 and A2. A mixture of felipeptins stimulated proliferation of cancer cells, while having no such effect on the normal cells. Detailed investigation revealed, that pre-treatment of cancer cells with a mixture of felipeptins resulted in downregulation of the tumor suppressor Rb, making the cancer cells to proliferate faster. Pre-treatment with felipeptins made cancer cells considerably more sensitive to the anticancer agent doxorubicin, and re-sensitized doxorubicin resistant cells to this drug. Structural characterization and binding experiments showed an interaction between felipeptins resulting in complex formation, which explains their synergistic effect. This discovery may open an alternative avenue in cancer treatment, helping to eliminate quiescent cells that often lead to cancer relapse.


## INTRODUCTION

Lasso peptides represent a family of ribosomally synthesized and post-translationally modified peptides, (RiPPs, Arnison et al., 2013; Maksimov et al., 2012; Hegemann et al., 2013; Tietz et al., 2017) whose biosynthetic gene clusters (BGCs) are present in many bacterial genomes (Hegemann et al., 2015; Mevaere et al., 2018). In recent years, peptide-based bioactive compounds have attracted considerable attention because of their high specificity to molecular targets and because they can relatively easy be re-designed by means of chemical synthesis and/or genetic engineering (Hegemann et al., 2019; de Veer et al., 2019; Pu et al., 2019; Habault and Poyet, 2019). Lasso peptides are small peptides (20 amino acids long, on average) of a unique “lasso” topology with the following features: (i) a macrolactam ring of 7-9 amino acid

residues established when the amino group of the N-terminus forms an isopeptide bond with the carboxyl side-chain of a glutamic or aspartic acid residue, (ii) the C-terminal tail trapped within the ring either by bulky amino acids or disulfide bridges, or both (Arnoson et al., 2013; Hegemann et al., 2015; Li et al., 2015a; Li et al., 2015b).

Lasso peptides are divided into four classes based on the number and position of disulfide bridges that are important structural features of these RiPPs (Tietz et al., 2017). Class I lasso peptides have two disulfide bridges that link the threaded tail above and below the macrolactam ring. Class II peptides have no disulfide bridges but have a "steric plug" composed of bulky amino acids on either side of the macrolactam ring to help stabilize the fold (Allen et al., 2016; Hegemann et al., 2016; Hegemann, 2020). Class III and IV have only one disulfide bridge. In class III the disulfide bridge links the tail to the macrolactam ring, whereas in class IV the disulfide bridge is located at the tail itself. So far only two class IV peptides have been characterized, LP2006 from the actinomycete bacterium *Nocardiopsis alba* (PDB accession number 5JPL; Tietz et al., 2017), and pandonodin from *Pandoraea norimbergensis* (PDB accession number 6Q1X; Cheung-Lee et al., 2019).

Bioactivities exhibited by lasso peptides are of definite interest in terms of drug discovery. Some bacterial lasso peptides, such as microcin J25 and capistruin, inhibit RNA polymerase in Gram-negative bacteria and thus have antibiotic activity (Braffman et al., 2019). Others act as antagonists of glucagon receptor (BI-32169; Knappe et al., 2010), endothelin B receptor (RES-701; Morishita et al., 1994) or have inhibitory activity in a cell invasion assay with cancer cells (sungsanpin; Um et al., 2013).

The minimal set of genes in a lasso peptide BGC encodes a precursor peptide (A) that contains an N-terminal leader and a C-terminal core region sequence, a leader peptide recognition protein (B1), a leader peptidase (B2) and a macrolactam synthase (C). Alternatively, many clusters

encode fused B1-B2 proteins. Furthermore, some lasso peptide BGCs can also contain genes for ABC transporters (D), isopeptidases or other additional modification enzymes (Hegemann et al., 2015; Tietz et al., 2017). Significant progress has recently been made in characterization of these proteins, as reported by Yan et al. (2012), DiCaprio et al. (2019), Choudhury et al. (2014), Fage et al. (2016), and Zhu et al. (2016). A study from 2017 provided good insight into the biosynthetic landscape of lasso peptides by identifying BGCs in available bacterial genomes and predicting a total of 1,315 lasso peptide sequences from them (Tietz et al., 2017). This number has nearly doubled in more recent work by de los Santos, who has developed a neural network for identification of RiPP precursor peptides (de los Santos, 2019). Chemical synthesis of lasso peptides is very difficult, and only one example has been reported recently (Chen et al., 2019), suggesting that the best way to produce such peptides and test their biological activities and potential as drug leads is to isolate them after biosynthesis in vivo.

The relatively small size of lasso peptide BGCs makes heterologous expression an attractive approach for the production of this class of compounds (Hegemann et al., 2013; Li et al., 2015b; Mevaere et al., 2018; Martin-Gomez et al., 2018). Vast majority of lasso peptides are of proteobacterial origin with only a few examples from actinomycetes. Except for the archetype lasso peptide J25 that was discovered in its native host, *Escherichia coli*, proteobacterial lasso peptides have typically been produced via heterologous expression. Sviceucin is the only lasso peptide from an actinomycete bacterium that has been produced via heterologous expression in considerably high quantities (Li et al., 2015a). Therefore, further attempts on expression of lasso peptide BGCs must be pursued in order to gain access to the diversity of lasso peptides, especially from actinomycete bacteria. This is particularly relevant for class IV lasso peptides, which are rare and poorly biologically characterized so far.

In this work, we present the successful genome mining of a newly isolated *Amycolatopsis* sp., leading to the heterologous expression, purification, structural and biological characterization of two class IV lasso peptides exhibiting unique synergistic biological activity, which may prove useful in combinational cancer chemotherapy.

## RESULTS AND DISCUSSION

***Amycolatopsis* sp. YIM10 metabolites and genome analyses.** *Amycolatopsis* sp. YIM10 was isolated from a rare earth mine of Bayan Obo, Inner Mongolia, China, and taxonomically identified by means of 16S rRNA gene sequencing. Cultivation of this isolate in different conditions revealed its ability to produce various tiglosides and 1,2,4-trimethoxynaphthalene, as suggested by LC-MS analyses (Figures S1-S4, Supplemental Information). While these natural products have been described previously (Guo et al., 2012; Rycroft et al., 1998), the latter has never been isolated from a bacterium before. The structures of these compounds were also confirmed using NMR spectroscopy (Figures S5-S6, Supplemental Information). No compounds with strong antimicrobial activity could be identified in these initial experiments. Keeping in mind the reported potential of *Amycolatopsis* spp. to produce bioactive secondary metabolites, the genome of YIM10 was completely sequenced (GenBank accession number CP045480, Table S3), and found to consist of a circular chromosome of 10.31 Mb and a 39.9 Kb plasmid. The genome was analyzed with antiSMASH 5.0 software (Blin et al., 2019), which identified at least 44 secondary metabolite BGCs. Several of these BGCs appear to be unique and could not be identified in the publicly available genomes of other bacteria (Table S4, Supplemental Information). The vast majority of BGCs identified in the genome of YIM10 had homologs in

the genome of recently described *Amycolatopsis albispora* WP1 isolated from marine sediment (Wu et al., 2018), suggesting that these strains are closely related.

Given that the genome of *Amycolatopsis* sp. YIM10 contains uncharacterized BGCs and therefore may have a potential to produce previously undescribed compounds, it was regarded as an excellent candidate for genome mining. First, this strain was evaluated as a possible subject for genetic manipulation. However, YIM10 was found to be resistant to all the antibiotics used as selection markers in actinomycetes, in particular apramycin, hygromycin, thiostrepton, kanamycin and puromycin. Thus, establishing a gene transfer system for this bacterium appeared problematic. Considering this, cloning and expression of BGCs in a heterologous host seemed like the only strategy to circumvent the problem. Therefore, a YIM10 fosmid genome library was constructed (Supplemental Information, Transparent Methods). We were particularly interested in expressing BGC21, which was predicted to govern biosynthesis of two class IV lasso peptides (MiBIG accession number BGC0002064). This BGC spans ~10 kb and contains all the main genes for the biosynthesis of this class of RiPPs.

Screening of the genome library using pooled PCR with primers designed for flanking and central regions of BGC21 led to the identification of a single fosmid containing the entire cluster. BGC21 (Figure 1) harbors two genes encoding precursor peptides (*filA1* and *filA2*), as well as genes for the proteins involved in the leader peptide recognition and cleavage (*filB1* and *filB2*), the macrolactam ring formation (*filC*), putative oxidoreductase-catalyzed reactions (*filE*), transport (*filD1* and *filD2*), and transcriptional regulation (*filR1*).

A cassette containing an *oriT* sequence and integration site int-attP$\varphi$C31 allowing conjugative transfer of the construct into *Streptomyces* bacteria and stable genomic integration, respectively, was incorporated into the identified fosmid using λ RED recombineering (Supplemental Information, Transparent Methods). The recombinant fosmid harboring BGC21 was introduced

into *Streptomyces coelicolor* M1154 engineered for heterologous expression of exogenous BGCs (Gomez-Escribano and Bibb, 2011) and *Streptomyces albus* J1074. The resulting recombinant strains were cultivated in different liquid and solid media, but no lasso peptide production could be detected in these conditions.

Next, the gene *filR1* encoding a transcriptional regulator of the SARP family, was cloned into the plasmid pSOK806 under control of the strong constitutive promoter ermEp* (Mevaere et al., 2018). The construct was conjugated into the abovementioned *Streptomyces* hosts that harbored integrated recombinant fosmid with BGC21. The constitutive overexpression of the FilR1 SARP regulator apparently triggered the production of both predicted lasso peptides in the two *Streptomyces* hosts when cultivated in liquid MYM medium (Figures S7-S8, Supplemental Information). The detected lasso peptides were designated felipeptins A1 and A2, and predicted, based on the sequence data, to be composed of 18 and 17 amino acids, respectively.

Given that the *S. coelicolor* M1154 host has a cleaner metabolic background compared to that of *S. albus* J1074, and virtually no differences in lasso peptides yields were found between the two strains (data not shown), it was decided to work further only with the former recombinant strain.

**Structure elucidation by LC-MS and NMR confirms the identity of two class IV lasso peptides.** Up-scaled fermentation and optimization of the purification protocol resulted in production yields of 12 mg/L of felipeptin A1, and 7 mg/L of felipeptin A2 (see Methods). These yields are significantly higher than those usually obtained after heterologous expression of lasso peptides BGCs (Li et al., 2015a; Mevaere et al., 2018; Martin-Gomez et al., 2018). Most likely, this is due to overexpression of the SARP regulator encoded by the felipeptins BGCs, which apparently controls expression of all other biosynthetic genes in the cluster. The measured molecular masses of felipeptin A1 (HRESIMS *m/z* 1009.4640 $[M+2H]^{2+}$; calculated for

$C_{91}H_{130}N_{26}O_{23}S_2^{2+}$, *m/z* 1009.4616, Δ = 2.4 ppm) and felipeptin A2 (HRESIMS *m/z* 922.9145 $[M+2H]^{2+}$; calculated for $C_{81}H_{119}N_{23}O_{23}S_2^{2+}$, *m/z* 922.9140, Δ = 0.5 ppm) matched well with the peptide sequences GSRGWGFEPGVRCLIWCD and GGGGRGYEYNKQCLIFC predicted from the *filA1* and *filA1* gene products, respectively, provided that two macrocycles are formed (Figure S8, Supplemental Information). The purity of felipeptins was verified using HPLC and LC-MS (Figures S9 and S10, Supplemental Information).

The structures of both felipeptins (Figure 2) were elucidated using an NMR-based approach, with DMSO as the solvent (see Methods). The structures depict an 18-mer peptide (felipeptin A1) and 17-mer peptide (felipeptin A2) with a looped-handcuff topology. Both peptides have an eight amino acid macrolactam ring at the N-terminus formed by condensation of the side-chain of Glu8 and the free N-terminus of Gly1. The formation of the isopeptide bond is confirmed by the long range nuclear Overhauser effect (NOE) peak between these two residues. For both felipeptins, threading of the loop region through the macrolactam ring is confirmed by the long-range NOEs ($H^{\alpha}$ Trp5–$H^{\alpha}$ Arg12 and $H^{N}$ Gly6–$H^{\alpha}$ Arg12). Formation of a disulfide bridge (Cys13-Cys17) in both felipeptins was confirmed by long-range NOEs between $H^{\alpha}$ of Cys17 and $H^{\beta}$ of Cys13. This disulfide bond might serve as a stabilizing feature by "trapping" the tail in position. Other structural features that might serve as steric locks are Val11 (in A1) and Gln12 (in A2) above the macrolactam ring, as well as Arg12 and Leu14 (in A1) and Leu14 (in A2) below the ring. The A1 and A2 structures have been deposited in the Protein Data Bank under the accession IDs 6XTH and 6XTI, respectively.

Structural features were also confirmed by the spectra of the two lasso peptides, obtained after tandem MS (Rosengren et al., 2004; Jeanne Dit Fouque et al., 2019),which showed a series of abundant a-, b-, and y-type peptide fragment ions covering the linear chain encompassing amino acids 9- 12. Their masses fit to the expected macrolactam ring formation between the N-terminal

Gly formed after removal of leader peptides and the side-chain of Glu8 on one side, as well as the formation of a second macrocycle via a disulfide bridge between Cys-residues in positions 13 and 17 (Figure 3).

**The proposed biosynthesis of the felipeptins A1 and A2 requires FilB1, FilB2, FilC and FilE for mature lasso peptide formation.** Based on the current knowledge on the functions of the lasso peptide biosynthesis enzymes, and the presence of a gene *filE* encoding an oxidoreductase, the biosynthesis of felipeptins was predicted as shown in Figure 4. According to the proposed biosynthetic pathway, the FilB1 protein recognizes the precursor peptides, products of *filA1* and *filA2* genes, and guides them to the peptidase FilB2, which cleaves off leader peptides (DiCaprio et al., 2019; Koos and Link, 2019). Immediately after cleavage, the lasso cyclase FilC forms a macrolactam ring and assists in the lasso fold formation. The last step in the biosynthesis is most likely accomplished by an oxidoreductase FilE, which forms disulfide bridges, stabilizing the final structures. Interestingly, database searches for proteins similar to FilE revealed only those with less than 55% identity, suggesting this oxidoreductase being rather unique.

Since the only other member of class IV lasso peptides biologically characterized, LP2006, displayed antibacterial activity, we tested felipeptins A1 and A2 against a panel of different Gram-positive bacteria in liquid media-based assays in order to determine minimal inhibitory concentrations. The results obtained suggest that felipeptins and their combination do not exhibit antibiotic properties, except in the cases of *Streptococcus pyogenes* and *Streptococcus pneumoniae*, where felipeptin A1 and the 1:1 A1+A2 mixture showed weak antibacterial activity (Table S5, Supplemental Information). Interestingly, in the case of *S. pyogenes*, only a mixture of felipeptins was found to be active. The synergistic effect was also clearly visible with the disk

diffusion assay performed using *Bacillus subtilis* as test organism (Figure S11, Supplemental Information).

**Felipeptins A1 and A2 exert a unique synergistic effect on cancer cells.** In order to evaluate other possible bioactivities of felipeptins A1 and A2, we tested the effect of a range of concentrations of felipeptins and their combination in cell viability assays using several cancer cell lines of different origin, including colon carcinoma HCT116, melanoma A375 and breast carcinoma MCF7, in comparison to normal cells, the human fibroblast cell line BJ and bone marrow-derived mesenchymal stem cells (MSC). While individual peptide treatments had marginal and statistically insignificant effects on the number of viable MCF7, HCT116 and A375 cells, their combination at certain ratios significantly increased the number of viable cancer cells in three cell lines (Figure 5A-C, left panels and Figure S12A-B). The effect of felipeptins combinations at several doses was synergistic, as shown in Figures 5A-C (green squares). In contrast, the effect of felipeptins on the growth rate of normal cells, BJ and MSC, was weak and without synergistic effect (Figure 5D and Figure S12C).

Since the increased number of cells could be due to either lower rate of cell death or higher rate of cell proliferation, we investigated the effect of felipeptins on cell cycle distribution using fluorescence-assisted cell sorting (FACS) of propidium-iodide stained cells (Figure 6A-C). While no change in the fraction of dead cells (subG1 fraction, <2N DNA content) could be observed, a decrease of cells in G1 (cell cycle preparatory phase, 2N DNA content) concomitantly with the increase of cells with >2N DNA content, i.e., cells in replication (S) and cell division (G2/M) phases was evident. These data clearly indicated an enhanced rate of proliferation.

To better understand the mechanism of pro-proliferative activity of felipeptins, we tested the involvement of tumor suppressors p53 and Rb, the two key factors that control the decisions of cells to proliferate (Hanahan and Weinberg, 2011). We addressed the involvement of p53 by using two cancer cell lines, MCF7p53KO and A375p53KO, in which the p53 gene was deleted by means of CRISPR-Cas9-mediated gene editing. However, the deletion of p53 did not significantly affect the pro-proliferative activity of felipeptins and their combinations (Figure S12D and E, Supplemental Information). Importantly, the observed statistically significant changes in the proportion of cells in different phases of the cell cycle, although minor, were qualitatively and quantitatively similar to those exhibited upon deletion of the gene for the retinoblastoma protein Rb (Brugarolas et al., 1998). In addition, we found a significant decrease in the level of the Rb protein and phosphorylated Rb upon felipeptin treatment in A375 cells, as assessed by immunoblotting (Figure 6D). Taken together, our data suggest that the inhibition of Rb is involved in stimulation of proliferation by felipeptins.

The concept that quiescent cancer stem-like cells (CSCs) within solid and hematological cancers confer resistance to chemo- and irradiation therapy, which preferentially targets rapidly proliferating cells, is currently widely accepted (Hanahan and Weinberg, 2011; Brown et al., 2017). Based on our data on stimulation of the cancer cell proliferation by felipeptins, we addressed the question of whether pre-treatment with felipeptins can increase the cytotoxic activity of the widely used chemotherapeutic drug doxorubicin (DOX). Importantly, we found that pre-treatment of MCF7 and A375 cells with felipeptins significantly and synergistically increased the efficiency of cancer cell suppression by doxorubicin (Figure 7A, B, left panels). The quantification of the synergistic effect of combination ratios is presented in the left panels In Figure 7 A, B (green squares). Further confirmation of the potentially beneficial effect of pre-treatment with felipeptins was obtained in a long-term (7 days) colony formation assay. In this

experiment, the A375 cells were pre-treated with a combination of 6.25 µM and 12.5 µM of felipeptins for 72h, followed by 72h DOX treatment. The number of cancer cell colonies was decreased much more efficiently by DOX upon pre-treatment with felipeptins (Figure 7C), demonstrating a remarkable increase in sensitivity towards DOX in comparison with the non-pretreated cells. Furthermore, the number of cells in the colonies was considerably lower in the felipeptins pre-treated samples. A number of studies have found that DOX has high propensity to select for drug-resistant cancer stem cells in previously differentiated cancer cells of various human solid tumors, including lung and breast carcinoma, neuroblastoma and osteosarcoma (Martins-Neves et al., 2018). Calcagno et al. have demonstrated that prolonged exposure of the MCF-7 breast cancer cells to doxorubicin selects for cells with a drug-resistant phenotype, enriched in stem cells with increased invasiveness and tumorigenicity (Calcagno et al., 2010). Following the previously described protocol (Calcagno et al., 2010), we selected DOX-resistant MCF7 cells and tested whether stimulation of their growth by felipeptins will overcome resistance to DOX (Figure 7D). As shown in Figure 7E, cells pre-treated with felipeptines were much more sensitive to the second treatment with DOX. Felipeptins decreased the number of drug-resistant colonies almost 4-fold. Moreover, as can be seen in Figure 7F, the remaining colonies contained fewer cancer cells, while the phenotype of some of those remaining cells (big, flat cells) suggests that they entered irreversible growth arrest (senescence), preventing their recurrent growth. Thus, our data demonstrate that stimulating the proliferation of drug-resistant cancer stem cells by felipeptins re-sensitized them to chemotherapy and overcame drug resistance.

Notably, the biological effect of combined felipeptins was dependent on the cell type. The selective effect of felipeptins on different types of cells lead us to speculate that the combination of felipeptins A1 and A2 might mimic a growth factor, hormone or cytokine, which are known to

have differential effects on different types of cells. For example, activin A, which belongs to the transforming growth factor beta superfamily, can exert both proliferative and anti-proliferative effects depending on the differentiation stage of the cell and the presence of other growth factors in the system (Bloise et al., 2019). Further high throughput studies are required to dissect the exact mechanism of the selective biological activity of felipeptins.

**Synergistic biological effect of felipeptins is likely due to complex formation.** In order to further investigate the synergistic effect between felipeptins A1 and A2, we performed an NMR titration experiment to measure the strength of the interaction (dissociation constant; $K_d$) between them (Supplemental Information). $^{13}$C-HSQC spectra of felipeptin A2 were recorded before and after addition of felipeptin A1. Upon increasing the concentration of felipeptin A1, we observed chemical shift perturbation in certain residues (side-chains of Arg5, Tyr7, Lys11 and Ile15; backbone of Lys11) in felipeptin A2. These affected residues were confirmed by chemical shift perturbations observed in a $^{15}$N-HSQC spectrum recorded at the end of the titration (Supplemental Information, Figure S12). These chemical shift perturbations indicate a change in the chemical environment of the observed $^{1}$H-$^{13}$C atom pairs that were used to estimate a $K_d$ = 0.3 ± 0.2 mM for the interaction (Figure S12). The amino acid specific locations of the highest chemical shift perturbations were used to guide the docking of felipeptins A1 and A2 using HADDOCK (van Zundert et al., 2016).

Figure S12 (Supplemental Information) shows a HADDOCK model, where the ring of one felipeptin interacts with the tail of the other (see figure text of Figure S12 for further discussion). While the NMR data fits best with a model in which felipeptins interact in a 1:1 ratio, we can't rule out the possibility of a model where felipeptins interact in other ratios. NMR studies were performed in DMSO due to the poor solubility of the felipeptins in water (see Transparent

Methods). While the observation of the interaction between felipeptins under these conditions does not entail the existence of an interaction under physiological conditions, it does not rule it out either.

Whatever the molecular mechanism behind the specific stimulation of cancer cell proliferation by felipeptins is, this unique biological activity may open interesting possibilities for combinational cancer therapy. Accumulated experimental evidence increasingly supports the notion that the persistence of quiescent subpopulations of cancer cells, including cancer stem cells (CSCs), cause relapse after initially successful chemotherapeutic treatment (Battle and Clevers, 2017). However, targeting quiescent CSCs remains a major challenge. A possible strategy could be to 'wake up' this cell population to increase its susceptibility to chemotherapy, as it has been demonstrated by genetic means in experimental models of chronic myeloid leukemia (Takeishi et al., 2013).

**Thermal and proteolytic stability of felipeptins.** Considering presumed potential of felipeptins in being used in therapy, it appeared necessary to test their thermal and proteolytic stability. To assess the thermal stability of the felipeptins and the stabilizing role of the disulfide bond, aqueous solutions were incubated at 95°C for 20h in the absence and presence of the reducing agent dithiothreitol (DTT). (Allen et al., 2016; Zong et al., 2017; Hegemann, 2020). Felipeptin A1 showed no sign of thermal unthreading after 20h at 95°C, even though partial hydrolytic cleavage of the C-terminal Asp18 was already observed. In the presence of DTT, not only reduction of the disulfide bond but also further chemical cleavage was detected, proving the stabilizing role of the disulfide bond (Fig. S14).

Felipeptin A2 also showed remarkable thermal stability, but the appearance of an additional peak in the chromatogram strongly indicated partial thermal unthreading after 20h at 95°C (Fig. S15).

The MS data for this additional peak proof identical mass and the MS/MS spectrum shows identical fragment ions that were, however, detected with altered relative intensities, indicating a different peptide fold (Fig. S16). Both peptides were stable towards carboxypeptides B and Y, which might as well be attributed to the lasso-fold (Fig. S17, S18) as well as to the disulfide bond close the C-terminus. Considering the size of the macrocycle formed by the disulfide bond (Fig. 2), it can be assumed that thermal unthreading proceeds via the tail pulling mechanism only, but which structural features determine the even higher stability of felipeptin A1 compared to A2 requires further detailed studies (Hegemann, 2020).

The high thermal and proteolytic stability observed for the felipeptins is definitely a big advantage when considering up-scaled biotechnological production and potential medical applications. Most of the current chemotherapeutic agents used for cancer treatment are designed to target rapidly dividing cancer cells, which are thus becoming more vulnerable to cytotoxic agents compared to normal cells. However, in many cases seemingly successful treatments of cancers still end up in relapse, owing to the dormant cancer cells that survive the treatment in a quiescent state. Pre-treatment of cancer cells with felipeptins sensitizes them to doxorubicin, a widely used chemotherapeutic agent, and may provide an opportunity to reduce the dosage of this cytotoxic agent and thereby minimize side effects. Moreover, pre-treatment of doxorubicin-resistant cancer cells with these lasso peptides makes them again sensitive to this drug. Taken together, our results suggest a possibility of an alternative direction in cancer therapy based on a combination of proliferation-inducing treatment and cytotoxic drugs targeting rapidly dividing cells.

**Limitations of the Study**

We note three limitations of this study. One relates to the exact mechanism of action of felipeptins on cancer cells, which appears to be due to the reduction in the amount of tumor suppressor protein Rb. However, how this reduction is achieved, and whether the felipeptins enter the cells or act on a membrane-anchored receptor is not known. Further studies, which would include more characterized cell lines, transcriptomics and proteomics can clarify this issue. The second limitation is due to the low solubility of lasso peptides in water, which prevented the studies on complex formation in the aqueous solutions mimicking cellular environment. Hence, only formation of the complex in DMSO-based solution could be shown. The third limitation relates to an idea of using the felipeptins in eukaryotic cell suspension cultures producing pharmaceutical proteins, where addition of lasso peptides could support more vigorous growth and hence increase the efficiency of the production process. This direction of research has not yet been addressed in the current study, but deserves proper investigation.

## Resource Availability

### Lead Contact

Further information and requests for bacterial strains, constructs and materials should be directed to the Lead Contact, Prof. Sergey B. Zotchev (sergey.zotchev@univie.ac,.at).

### Materials Availability

Data related to this paper may be requested from the lead author. The bacterial strains isolated, constructed and examined in this study can be requested from the Lead Contact.

### Data and Code Availability

The genome sequence of *Amycolatopsis* sp. YIM10 is available in GenBank under accession number CP045480.1. Chemical shift assignments of felipeptins A1 and A2 have been deposited in the BMRB under the accession codes 34478 and 34479, respectively. NMR ensemble structures of felipeptin A1and A2 are deposited in the Protein database under accession numbers 6TXH and 6TXI, respectively.

**Methods**

All methods can be found in the accompanying Transparent Methods supplemental file.

**ACKNOWLEDGEMENTS**

This study was supported by the University of Vienna, Swedish Research Council, Swedish Cancer Society, Bielefeld University, the University of Yunnan, NTNU Norwegian University of Science and Technology and the grants from the Novo Nordisk Foundation (NNF18OC0032242) and the Norwegian Research Council (226244, 269408). We also acknowledge support by the Mass Spectrometry Centre of the Faculty of Chemistry, University of Vienna.

**AUTHOR CONTRIBUTIONS**

SBZ, GS, GC, EM, FLA designed research; JFGG, MZ, MS, SR, EU, YRC, YJ,GC, EM, FLA performed research; MZ, EU, CR, TB, JK, CJ, GS, MS, GC, EM, FLA analyzed data; CJ provided research material; SBZ, GS, MS, MZ, CJ, GC, EM, FLA wrote the paper.

**DECLARATION OF INTEREST**

Authors declare no competing interest.

## SUPPLEMENTAL INFORMATION

Transparent Methods, Supplemental figures, and Supplemental tables.

## REFERENCES

Allen, C.D., Chen, M.Y., Trick, A.Y., Le, D.T., Ferguson, A.L., and Link, A.J. (2016). Thermal Unthreading of the Lasso Peptides Astexin-2 and Astexin-3. ACS Chem. Biol. *11*, 3043-3051.

Arnison, P.G., Bibb, M.J., Bierbaum, G., Bowers, A.A., Bugni, T.S., Bulaj, G., Camarero, J.A., Campopiano, D.J., Challis, G.L., Clardy, J., et al. (2013) Ribosomally synthesized and post-translationally modified peptide natural products: overview and recommendations for a universal nomenclature. Nat. Prod. Rep. *30*, 108−160.

Batlle, E. and Clevers, H. (2017) Cancer stem cells revisited. Nat. Med. *23*, 1124–1134.

Blin, K., Shaw, S., Steinke, K., Villebro, R., Ziemert, N., Lee, S.Y., Medema, M.H., and Weber, T. (2019) antiSMASH 5.0: Updates to the Secondary Metabolite Genome Mining Pipeline. Nucleic Acids Res. *47*, W81-W87.

Bloise, E., Ciarmela, P., Dela Cruz, C., Luisi, S., Petraglia F., and Reis, F.M. (2019) Activin A in Mammalian Physiology. Physiol. Rev. *99*, 739-780.

Braffman, N.R., Piscotta, F.J., Hauver, J., Campbell, E.A., Link, A.J. and Darst, S.A. (2019) Structural mechanism of transcription inhibition by lasso peptides microcin J25 and capistruin. Proc Natl. Acad. Sci. U S A *116*, 1273-1278.

Bredholdt, H., Galatenko, O.A., Engelhardt, K., Fjaervik, E., Terekhova, L.P., and Zotchev, S.B. (2007) Rare actinomycete bacteria from the shallow water sediments of the Trondheim fjord, Norway: isolation, diversity and biological activity. Environ. Microbiol. *9***,** 2756-2764.

Brown, J.A., Yonekubo, Y., Hanson, N., Sastre-Perona, A., Basin, A., Rytlewski, J.A., Dolgalev, I., Meehan, S., Tsirigos, A., Beronja, S., et al. (2017) TGF-β-Induced Quiescence Mediates Chemoresistance of Tumor-Propagating Cells in Squamous Cell Carcinoma. Cell Stem Cell. *21*, 650–664.

Brugarolas, J., Bronson, R.T. and Jacks, T.J. (1998) p21 Is a Critical CDK2 Regulator Essential for Proliferation Control in Rb-deficient Cells. Cell Biol. *141*, 503–514.

Calcagno, A.M., Salcido, C.D., Gillet, J.P., Wu, C.P., Fostel, J.M., Mumau, M.D., Gottesman, M.M., Varticovski, L., and Ambudkar, S.V. (2010) Prolonged Drug Selection of Breast Cancer Cells and Enrichment of Cancer Stem Cell Characteristics. J. Natl. Cancer Inst. *102*, 1637-1652.

Chen, M., Wang, S. and Yu, X. (2019) Cryptand-imidazolium sup-ported total synthesis of the lasso peptide BI-32169 and its d-enantiomer. Chem. Commun. *55*, 3323-3326.

453 Cheung-Lee, W.L., Cao, L., Link, A.J. and Pandonodin, A. (2019) Proteobacterial Lasso Peptide
454 With an Exceptionally Long C-Terminal Tail. ACS Chem. Biol. *14*, 2783-2792.
455
456 Choudhury, H.G., Tong, Z., Mathavan, I., Li, Y., Iwata, S., Zirah, S., Rebuffat, S., van Veen,
457 H.W., and Beis, K. (2014). Structure of an antibacterial peptide ATP-binding cassette transporter
458 in a novel outward occluded state. Proc. Natl. Acad. Sci. U S A. *111*, 9145-9150.
459
460 de los Santos, E.L.C. (2019) NeuRiPP: Neural network identi-fication of RiPP precursor
461 peptides. Sci. Rep. *9*, 13406.
462
463 de Veer, S.J., Kan, M.W., and Craik, D.J. (2019) Cyclotides: From Structure to Function. Chem
464 Rev. *119*, 12375-12421.
465
466 DiCaprio, A.J., Firouzbakht, A., Hudson, G.A., and Mitchell, D.A. (2019). Enzymatic
467 Reconstitution and Biosynthetic Investigation of the Lasso Peptide Fusilassin. J. Am. Chem. Soc.
468 *141*, 290-297.
469
470 Di Veroli GY, Fornari C, Wang D, Mollard S, Bramhall JL, Richards FM, Jodrell DI. (2016)
471 Combenefit: An Interactive Platform for the Analysis and Visualization of Drug Combinations.
472 Bioinformatics *32*, 2866-2868.
473
474 Essmann, U., Perera, L., and Berkowitz, M.L. (1995) A smooth particle mesh Ewald method. J.
475 Chem. Phys. *103*, 8577-8593.
476

Fage, C.D., Hegemann, J.D., Nebel, A.J., Steinbach, R.M., Zhu, S., Linne, U., Harms, K., Bange, G., and Marahiel, M.A. (2016). Structure and Mechanism of the Sphingopyxin I Lasso Peptide Isopeptidase. Angew. Chem. Int. Ed. Engl. *55*, 12717-12721.

Flett, F., Mersinias, V., and Smith, C.P. (1997) High efficiency intergeneric conjugal transfer of plasmid DNA from Escherichia coli to methyl DNA-restricting streptomycetes. FEMS Microbiol. Lett. *155***,** 223-229.

Gomez-Escribano, J. P., and Bibb, M. J. (2011) Engineering *Streptomyces coelicolor* for heterologous expression of secondary metabolite gene clusters. Microb. Biotechnol. *4*, 207-215.

Guo, Z.K., Zhang, G.F., Jiao, R.H., Shen, Y., Xu, Q., Tan, R.X., and Ge, H.M. (2012) Actinotetraoses A-H: Tetrasaccharide Derivatives From a Grasshopper-Associated *Amycolatopsis* sp. HCa1. Planta Med. *78*, 988-994.

Gordon, D., and Green, P. (2013) Consed: a graphical editor for next-generation sequencing. Bioinformatics *29***,** 2936-2937.

Gust, B. (2009) Chapter 7. Cloning and analysis of natural product pathways. Methods Enzymol. *458***,** 159-180.

Güntert, P. (2004) Automated NMR structure calculation with CYANA. Methods Mol. Biol. *278*, 353–378.

501 Hanahan, D., and Weinberg, R.A. (2011) Hallmarks of Cancer: The Next Generation. Cell *144*,
502 646-674.
503
504 Habault, J., and Poyet, J.L. (2019) Recent Advances in Cell Pene-trating Peptide-Based
505 Anticancer Therapies. Molecules *24*, pii: E927.
506
507 Hegemann, J.D. (2020). Factors Governing the Thermal Stability of Lasso Peptides.
508 Chembiochem. *21*, 7-18.
509
510 Hegemann, J.D., Zimmermann, M., Zhu, S., Klug, D., and Marahiel, M.A. (2013). Lasso
511 peptides from proteobacteria: Genome mining employing heterologous expression and mass
512 spectrometry. Biopolymers. *100*, 527-542.
513
514
515 Hegemann, J.D., Fage, C.D., Zhu, S., Harms, K., Di Leva, F.S., Novellino, E., Marinelli, L., and
516 Marahiel, M.A. (2016). The ring residue proline 8 is crucial for the thermal stability of the lasso
517 peptide caulosegnin II. Mol. Biosyst. *12*, 1106-1109.
518
519 Hegemann, J.D., Bobeica, S.C., Walker,M.C., Bothwell, I.R., and van der Donk, W.A. (2019).
520 Assessing the Flexibility of the Prochlorosin 2.8 Scaffold for Bioengineering Applications. ACS
521 Synth. Biol. *8*, 1204-1214.
522
523 Israel, D.I. (2006) PCR-Based Screening of DNA Libraries. CSH Protoc. *2006(1)*, pdb.prot4129.
524

Jeanne Dit Fouque, K., Bisram, V., Hegemann, J.D., Zirah, S., Rebuffat, S., and Fernandez-Lima, F. (2019). Structural signatures of the class III lasso peptide BI-32169 and the branched-cyclic topoisomers using trapped ion mobility spectrometry-mass spectrometry and tandem mass spectrometry. Anal. Bioanal. Chem. *411*, 6287-6296.

Keller, R. (2004) The Computer Aided Resonance Assignment Tutorial, CANTINA Verlag, Goldau, Switzerland.

Knappe, T.A., Linne, U., Xie, X., and Marahiel, M.A. (2010) The glucagon receptor antagonist BI-32169 constitutes a new class of lasso peptides. FEBS Lett. *584*, 785-789.

Koos, J.D., and Link, A.J. (2019). Heterologous and in Vitro Reconstitution of Fuscanodin, a Lasso Peptide from *Thermobifida fusca*. J. Am. Chem. Soc. *141*, 928-935.

Krieger, E., Koraimann, G., and Vriend, G. (2002). Increasing the precision of comparative models with YASARA NOVA--a self-parameterizing force field. Proteins *47*, 393-402.

Krishnamoorthy, J., Yu, V.C., and Mok, Y.K. (2010) Auto-FACE: an NMR based binding site mapping program for fast chemical exchange protein-ligand systems. PLoS ONE *5*, e8943.

Li, Y., Ducasse, R,. Zirah, S., Blond, A., Goulard, C., Lescop, E., Giraud, C., Hartke, A., Guittet, E., Pernodet, J.L., and Rebuffat, S. (2015a) Characterization of Sviceucin from *Streptomyces*

548 Provides Insight into Enzyme Exchangeability and Disulfide Bond Formation in Lasso Peptides.
549 ACS Chem. Biol. *10*, 2641-2649.
550
551 Li, Y., Zirah, S., and Rebuffat, S. (2015b) Lasso Peptides. Bacterial Strategies to Make and
552 Maintain Bioactive Entangled Scaffolds, Springer, New York.
553
554 Maksimov, M.O., Pelczer, I., and Link, A.J. (2012). Precursor-centric genome-mining approach
555 for lasso peptide discovery. Proc Natl Acad Sci U S A. *109*, 15223-15228.
556
557 Martin-Gómez, H., Linne, U., Albericio, F., Tulla-Puche, J., and Hegemann, J.D. (2018).
558 Investigation of the Biosynthesis of the Lasso Peptide Chaxapeptin Using an *E. coli*-Based
559 Production System.
560 J. Nat. Prod. *81*, 2050-2056.
561
562 Martins-Neves, S.R., Cleton-Jansen, A.M., and Gomes, C.M.F. (2018) Therapy-induced
563 enrichment of cancer stem-like cells in solid human tumors: Where do we stand? Pharmacol.
564 Res. *137*, 193–204.
565
566 Mevaere, J., Goulard, C., Schneider, O., Sekurova, O.N., Ma, H., Zirah, S., Afonso, C., Rebuffat,
567 S., Zotchev, S.B., and Li, Y. (2018) An orthogonal system for heterologous expression of
568 actinobacterial lasso peptides in *Streptomyces* hosts. Sci. Rep. *8*, 8232.
569
570 Morishita, Y., Chiba, S., Tsukuda, E., Tanaka, T., Ogawa, T., Yamasaki, M., Yoshida, M.,
571 Kawamoto, I., and Matsuda, Y. (1994) RES-701-1, a novel and selective endothelin type B

receptor antagonist produced by *Streptomyces* sp. RE-701. I. Characterization of producing strain, fermentation, isolation, physico-chemical and biological properties. J. Antibiot. **47**, 269–275.

Peuget, S., Zhu, J., Sanz, G., Singh, M., Gaetani, M., Chen, X., Shi, Y., Saei, A.A., Visnes, T., Lindström, M.S. et al. (2020) Thermal Proteome Profiling Identifies Oxidative-Dependent Inhibition of the Transcription of Major Oncogenes as a New Therapeutic Mechanism for Select Anticancer Compounds. Cancer Res. *80*, 1538-1550.

Pu, J., Wang, Q., Xu, W., Lu, L., and Jiang, S. (2019) Development of Protein- And Peptide-Based HIV Entry Inhibitors Targeting gp120 or gp41. Viruses *11*, pii: E705.

Rosengren, K.J., Blond, A., Afonso, C., Tabet, J.C., Rebuffat, S., and Craik, D.J. (2004). Structure of thermolysin cleaved microcin J25: extreme stability of a two-chain antimicrobial peptide devoid of covalent links. Biochemistry. *43*, 4696-702.

Rycroft, D.S., Cole, W.J., and Rong, S. (1998) Highly oxygenated naphthalenes and acetophenones from the liverwort *Adelanthus decipiens* from the British isles and south America. Phytochemistry *48*, 1351-1356.

Seemann, T. (2014) Prokka: Rapid Prokaryotic Genome Annotation. Bioinformatics *30***,** 2068-2069.

595 Sekurova, O.N., Zhang, J., Kristiansen, K.A., and Zotchev, S.B. (2016) Activation of
596 Chloramphenicol Biosynthesis in *Streptomyces venezuelae* ATCC 10712 by Ethanol Shock:
597 Insights From the Promoter Fusion Studies. Microb. Cell Fact. *15***,** 85.
598
599 Takeishi, S., Matsumoto, A., Onoyama, I., Naka, K., Hirao, A., and Nakayama, K.I. (2013)
600 Ablation of Fbxw7 eliminates leukemia-initiating cells by preventing quiescence. Cancer Cell
601 *23*, 347–361.
602
603 Tietz, J.I., Schwalen, C.J., Patel, P.S., Maxson, T., Blair, P.M., Tai, H.C., Zakai, U.I., Mitchell,
604 D.A. (2017) A new genome-mining tool redefines the lasso peptide biosynthetic landscape. Nat.
605 Chem. Biol. *13*, 470-478.
606
607 Um, S., Kim, Y.J., Kwon, H., Wen, H., Kim, S.H., Kwon, H.C., Park, S., Shin, J., and Oh, D.C.
608 (2013) Sungsanpin, a lasso pep-tide from a deep-sea streptomycete. J. Nat. Prod. *76*, 873-879.
609
610 van Zundert, G.C.P., Rodrigues, J.P.G.L.M., Trellet, M., Schmitz, C., Kastritis, P.L., Karaca, E.,
611 Melquiond, A.S.J., van Dijk, M., de Vries, S.J., and Bonvin, A.M.J.J. (2016) The HADDOCK2.2
612 Web Server: User-Friendly Integrative Modeling of Biomolecular Complexes. J. Mol. Biol. *428*,
613 720-725.
614
615 Wu, Q., Deering, R.W., Zhang, G., Wang, B., Li, X., Sun, J., Chen, J., Zhang, H., Rowley, D.C.,
616 and Wang, H. (2018) Albisporachelin, a New Hydroxamate Type Siderophore from the Deep
617 Ocean Sediment-Derived Actinomycete *Amycolatopsis albispora* WP1T. Mar. Drugs *16*, pii:
618 E199.

Yan, K.P., Li, Y., Zirah, S., Goulard, C., Knappe, T.A., Marahiel, M.A., and Rebuffat, S. (2012). Dissecting the maturation steps of the lasso peptide microcin J25 in vitro. Chembiochem. *13*, 1046-1052.

Zhu, S., Hegemann, J.D., Fage, C.D., Zimmermann, M., Xie, X., Linne, U., and Marahiel, M.A. (2016). Insights into the Unique Phosphorylation of the Lasso Peptide Paeninodin. J. Biol. Chem. *291*, 13662-13678.

Zong, C., Wu, M.J., Qin, J.Z., and Link, A.J. (2017). Lasso Peptide Benenodin-1 Is a Thermally Actuated [1]Rotaxane Switch. J. Am. Chem. Soc. *139*, 10403-10409.

## FIGURE LEGENDS

**Figure 1.** Lasso peptide biosynthesis gene cluster from *Amycolatopsis* sp. YIM10: organization of genes and predicted functions of their products.

**Figure 2.** NMR ensemble structures of (A) felipeptin A1 PDB:6TXH and (B) A2 PDB:6TXI. The structures depict the looped-handcuff topology stabilized by a disulfide bridge, characteristic of class IV lasso peptides. In both structures, amino-acids G1-E8 in the macrolactam ring are colored lighter, and the disulfide bridges, C13-C17, are colored yellow. The amino acid sequences and lowest energy conformers for felipeptins A1 (C) and A2 (D) are also shown.

**Figure 3.** HRESIMS/MS spectra of the [M+2H]2+ ions of felipeptin A1 at m/z 1009.4640 (A) and felipeptin A2 at m/z 922.9145 (B). The fragmentation, occurring mainly in the linear region between the two macrocycles, fully confirms the structures predicted from the BGC data.

643 **Figure 4.** Proposed felipeptins biosynthesis pathway.

644 **Figure 5.** Synergistic induction of cancer cell proliferation by felipeptins. (A-D) Left panels,
645 heatmaps show changes of the number of viable cells upon 72 h treatment with different doses of
646 felipeptins and their combinations at a 2-fold serial dilution (as indicated in the figures) in cancer
647 cell lines MCF7 (A), A375 (B), HCT116 (C) and normal cells, BJ fibroblasts and bone marrow-
648 derived mesenchymal stem cells MSC (D), measured using rezasurin assay and normalized to
649 DMSO control. Red indicates increased cell number, white – no change, blue – decreased cell
650 number. Right panels, heatmaps show Highest Single Agent (HSA) reference model score,
651 indicated by green color (A-D). Data presented as mean log2 from two independent experiments
652 performed in duplicate.

653 **Figure 6**. Felipeptins stimulate proliferation of cancer cells via inhibition of pRb. (A, C)
654 Stimulation of cell cycle progression by 24h treatment with felipeptins (green bars, 6.25 μM
655 each; red bars, 12.5 μM each) as detected by FACS of propidium iodide-stained A375 (A, B) and
656 HCT116 (C) cell lines. Grey bars, control DMSO treatment. Data shown as mean ± SD from two
657 independent experiments. *$p<0.05$, unpaired t test. (D) Western blotting for total RB and
658 phospho-Rb in A375 upon felipeptins treatment for 24 h. β-Actin is used as a loading control.

659 **Figure 7**. Felipeptins sensitize cancer cells to doxorubicin and overcome drug resistance of
660 cancer stem cells. (A,B) Heatmaps (left panels) reflect the number of viable cells in A375 (A)
661 and MCF7 (B) cell lines, pre-treated with different concentrations of felipeptins for 72h followed
662 by doxorubicin for another 72h. HAS Synergy scores (right panels) are indicated in green color.
663 Data presented as mean log2 from two independent experiments performed in duplicate. (C)
664 Long-term viability assay (7-day colony formation) in A375 cells, pre-treated or not pre-treated
665 with felipeptins A1+A2 before applying doxorubicin as in (A). Colonies were detected using
666 crystal violet staining. The charts illustrate the percentage of the colony numbers relative to the

667 untreated control. ** 0.01 ≤ p. (D). Schematic illustration of the experiment. I -Doxorubicin-
668 resistant MCF-7 cancer stem cells were obtained upon 72h treatment by 12.5 nM doxorubicin. II-
669 Their growth was stimulated by combination of felipeptins (25 μM each) for 96 h. III- Resulting
670 colonies were treated by the same doses of DOX or felipeptins or Dox/felipeptins combination
671 for 5 days. (E) Quantification of drug-resistant colonies obtained as in (D) upon treatment of
672 DOX or felipeptins or their combination. Colonies were detected using crystal violet staining;
673 colonies were counted using image J analysis. (F) Representative phase-contrast microscopy
674 image of crystal violet-stained colonies obtained as shown in (D).

**Figure 1.** Lasso peptide biosynthesis gene cluster from Amycolatopsis sp. YIM10: organization of genes and predicted functions of their products.

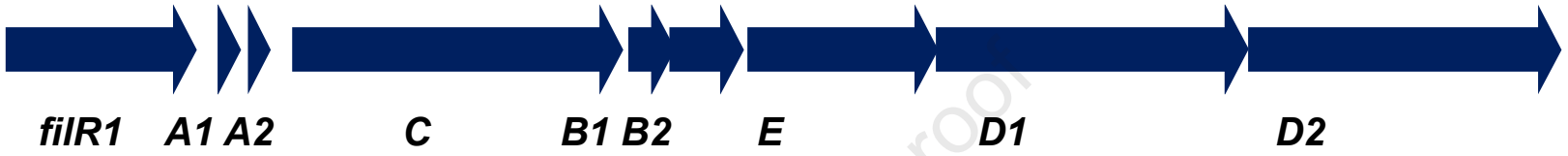


| Gene | Gene product |
|---|---|
| *filR1* | transcriptional regulator (SARP family) |
| *filA1* | felipeptin A1 lasso peptide precursor |
| *filA2* | felipeptin A2 lasso peptide precursor |
| *filC* | asparagine synthase (lasso cyclase) |
| *filB1* | PqqD family protein (leader peptide binding) |
| *filB2* | transglutaminase-like superfamily protein (leader peptidase) |
| *filE* | LLM class flavin-dependent oxidoreductase (disulfide bridge formation) |
| *filD1* | ABC transporter (lasso peptide efflux) |
| *filD2* | ABC transporter (lasso peptide efflux) |

**Figure 2.** NMR ensemble structures of ellipeptins A1 and A2.

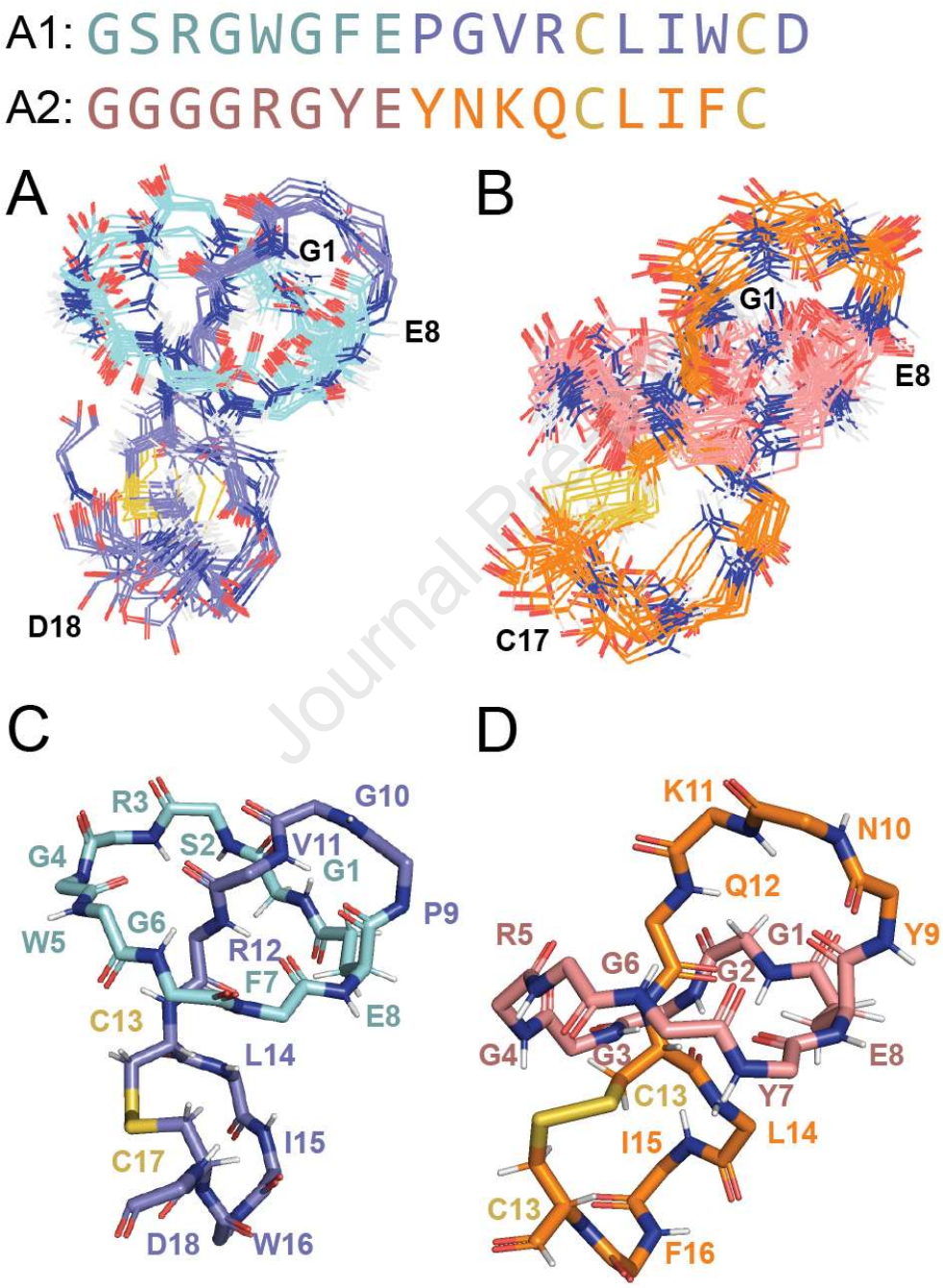

**Figure .** R SIMS MS spectra of [redacted] A and felipeptin A2 at m 22. 1 B .

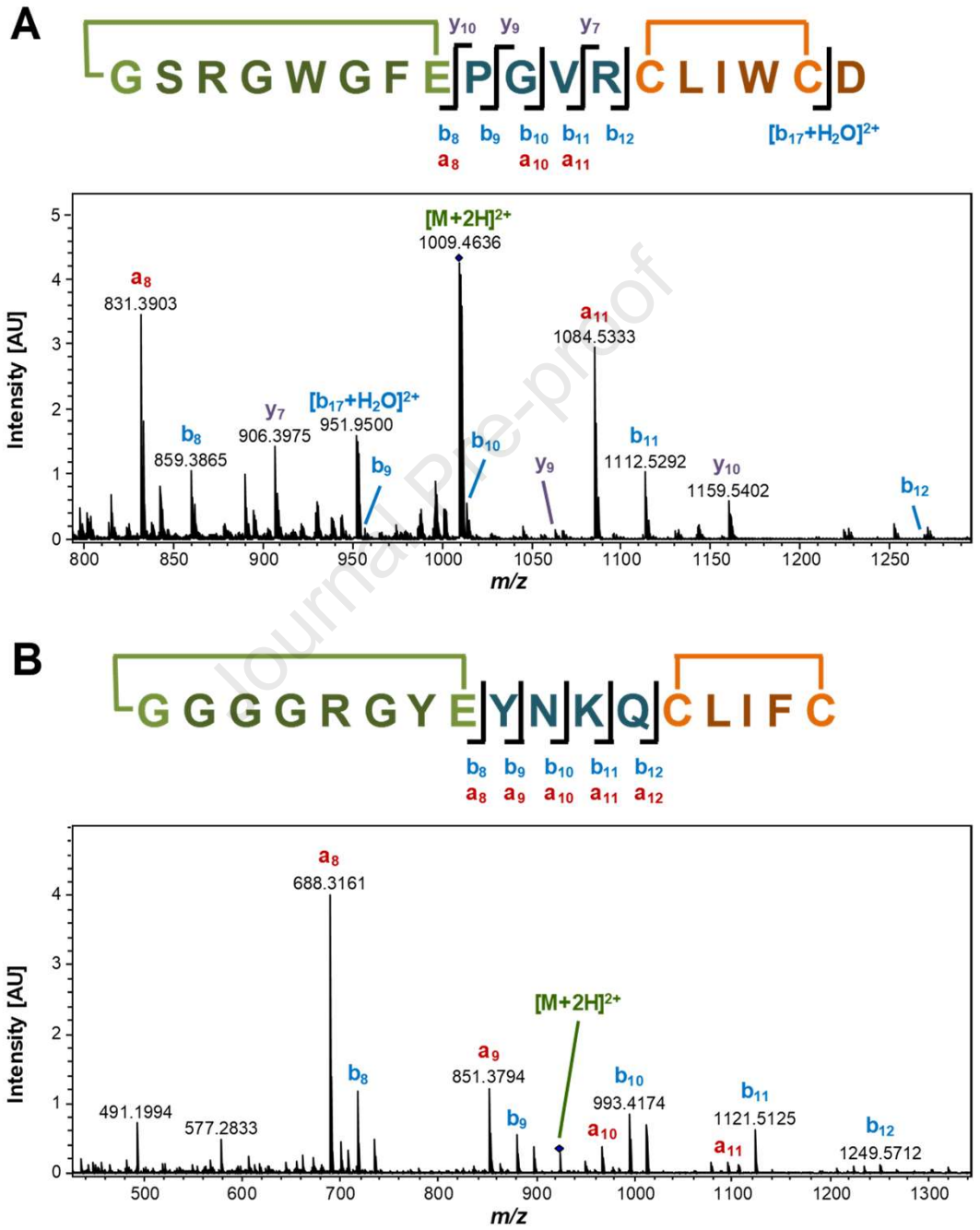

***Fi r*** Proposed felipeptins biosynthesis pathway.

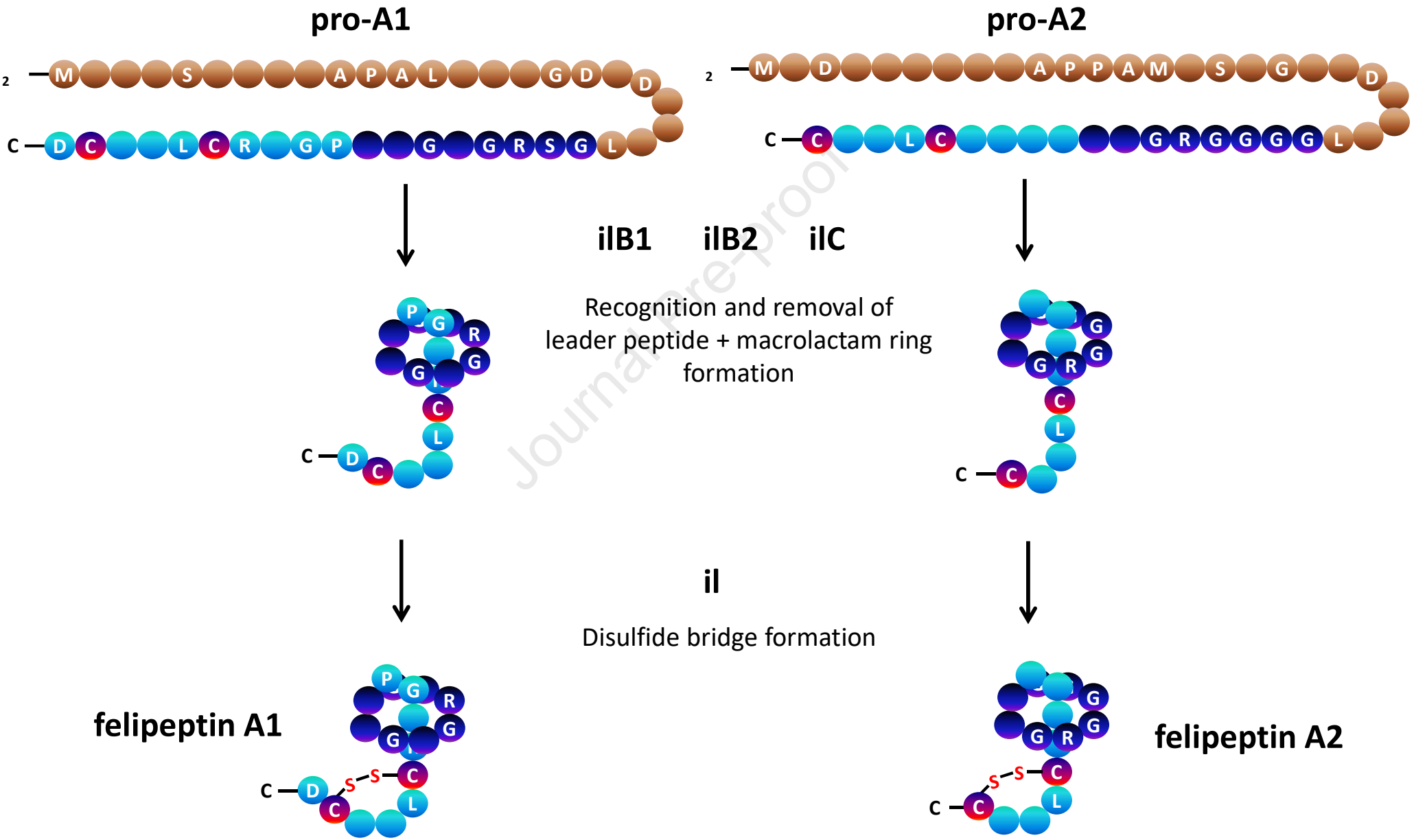

**Figure .** S ner istic induction of cancer cell proliferation b fellpeptins.

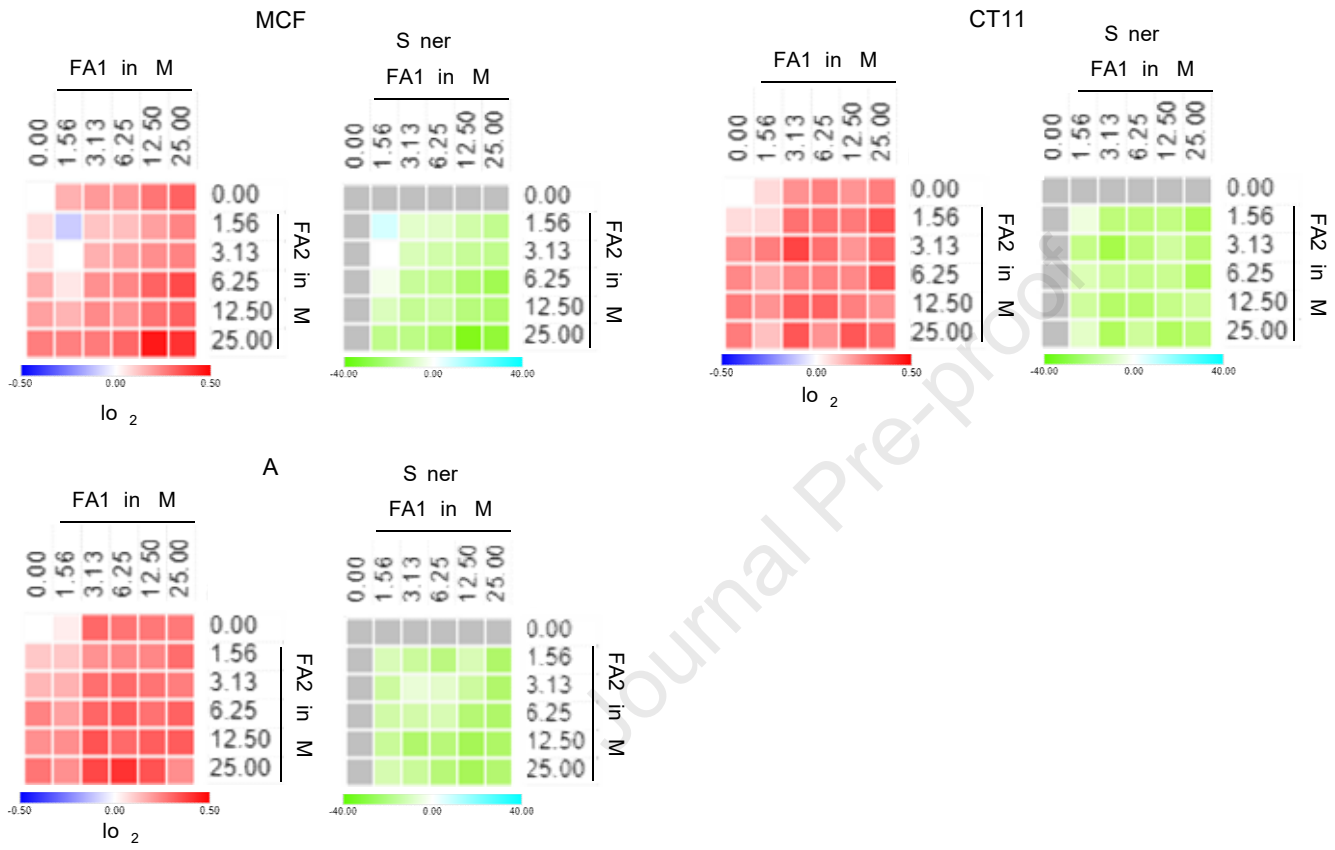


**D**

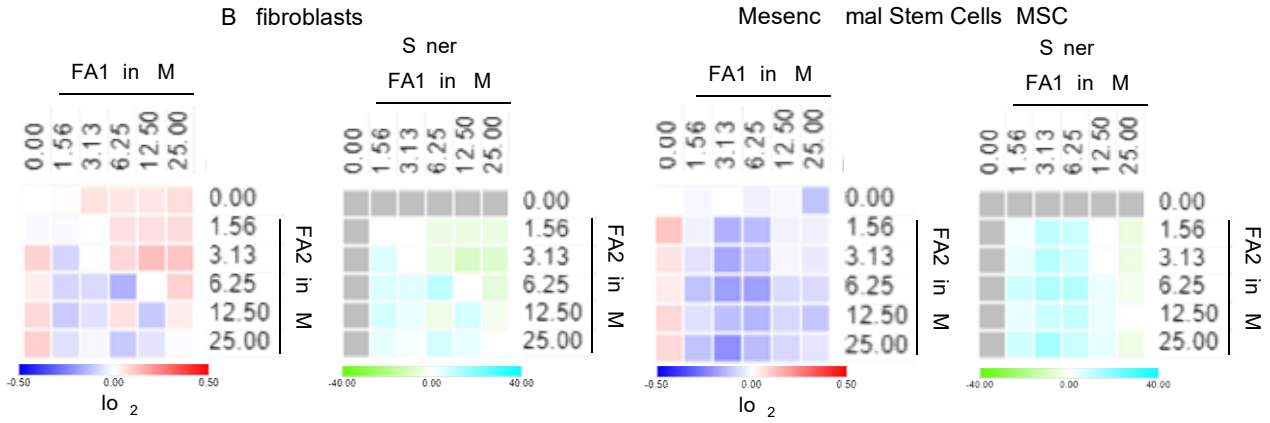

**Figure .** Felipeptins stimulate proliferation of cancer cells via inhibition of pRb.

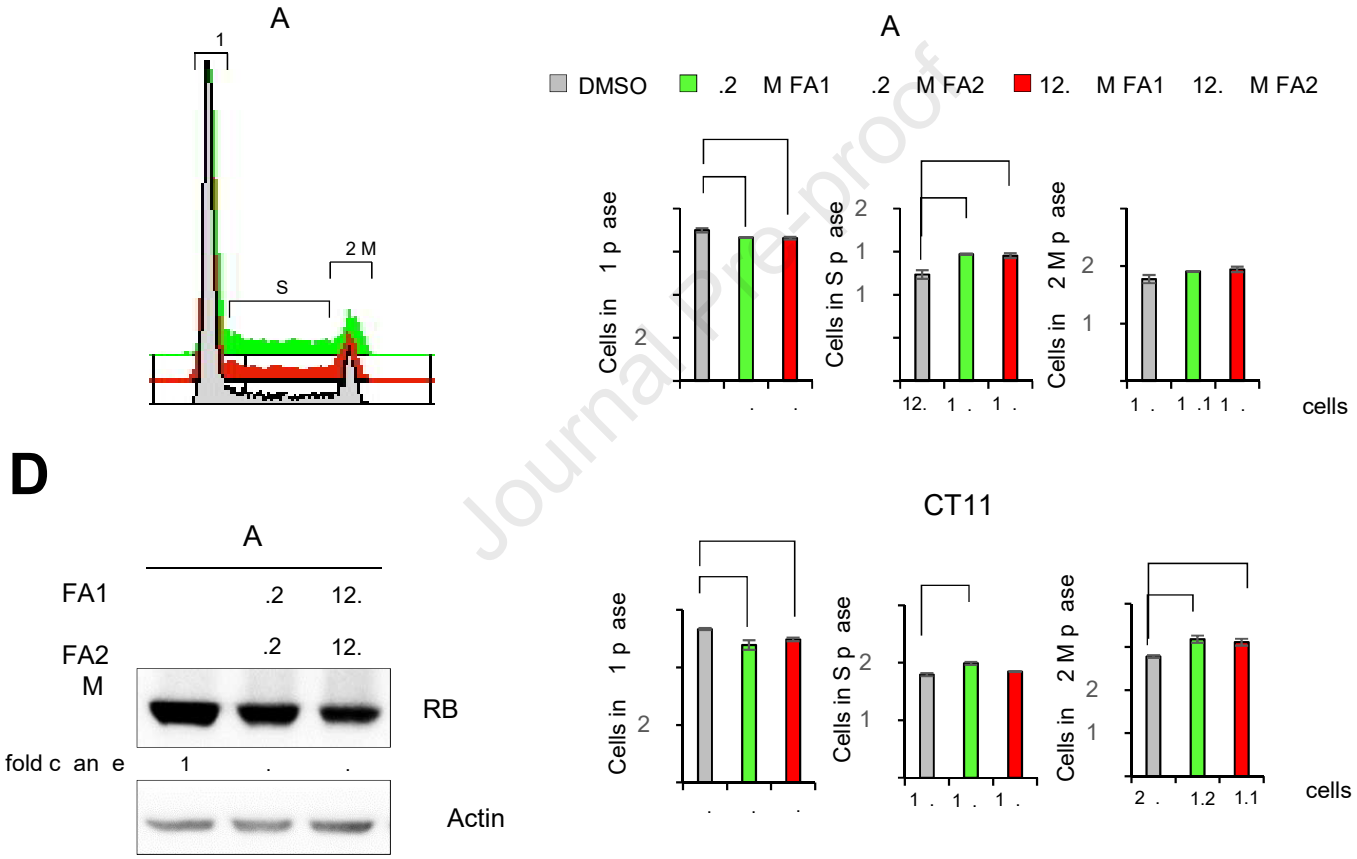

**Figure 7.** Felipeptins sensitize can[Journal Pre-proof]ce of cancer stem cells.

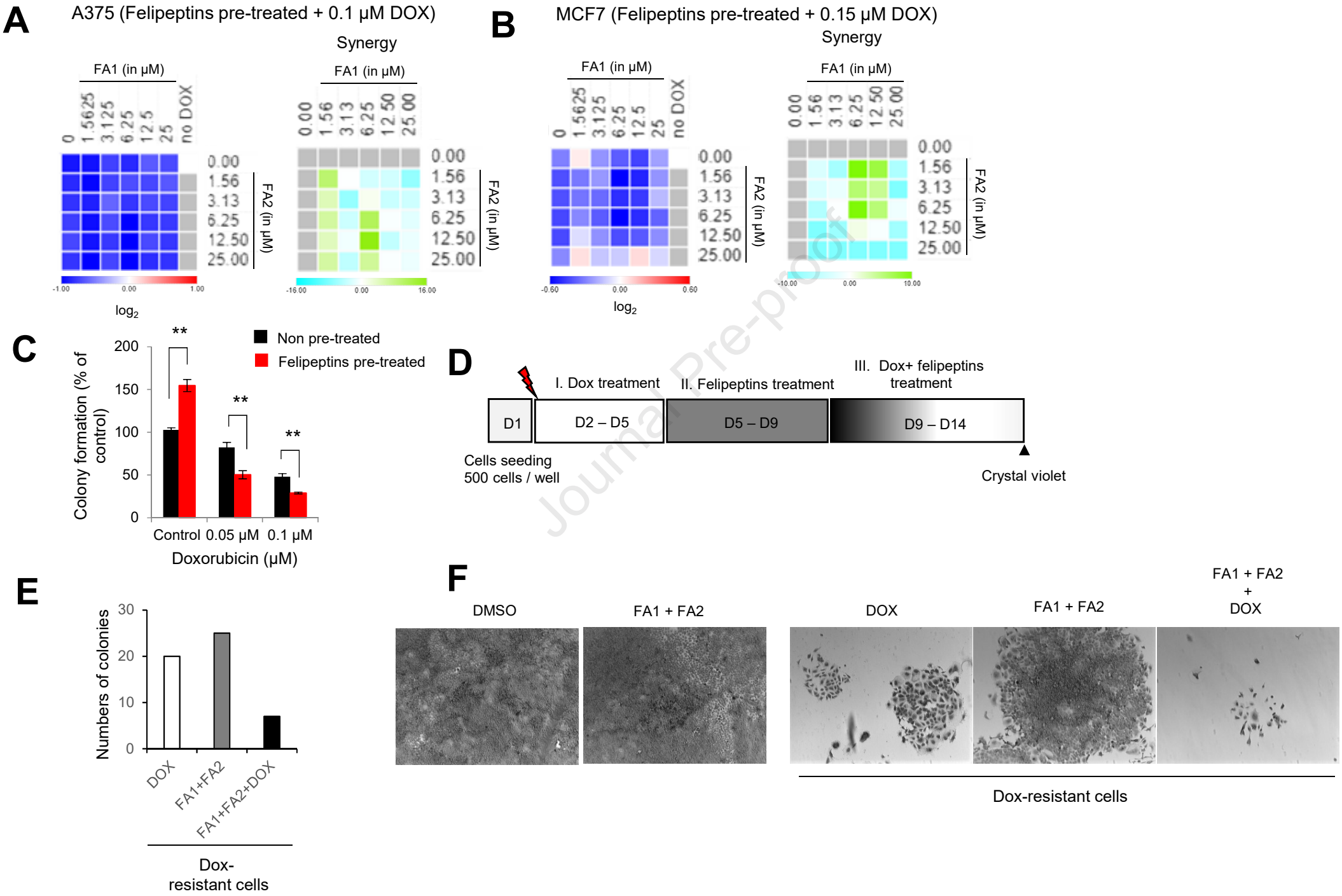

# Class IV lasso peptides synergistically induce proliferation of cancer cells and sensitize them to doxorubicin

Jaime Felipe Guerrero-Garzón[1,‡], Eva Madland[2,‡], Martin Zehl[3], Madhurendra Singh[4], Shiva Rezaei[4,5], Finn L. Aachmann[2], Gaston Courtade[2], Ernst Urban[6], Christian Rückert[7], Tobias Busche[7], Jörn Kalinowski[7], Yan-Ru Cao[8], Yi Jiang[8], Cheng-lin Jiang[8], Galina Selivanova[4]*, Sergey B. Zotchev[1]*

## Highlights

- Lasso peptides felipeptins from *Amycolatopsis* sp. produced in a heterologous host
- Felipeptins synergistically sensitize cancer cells to doxorubicin
- Synergistic effect on cancer cells appears to be due to complex formation
- Felipeptins overcome drug resistance of cancer stem cells